Copyright © 2012 Tech Science Press SL, vol.7, no.3, pp.167-185, 2012

Studies on Ring Compression Test using Finite Element Analysis on Sintered Aluminium Alloys

B. Ramesh, and T. Senthilvelan

Abstract: Friction factor plays decisive role in the overall integrity of metal forming processes. As the friction during deformation influences the applied load, product shape, surface quality, internal structure, it is of paramount importance to know its influential parameters .In this investigation, the friction factor at unlubricated and Lubricated conditions with SAE 40 oil, Molydenum Disulphide, Graphite as lubricant at different temperatures has been analyzed. Among the lubricant, it is found that molybdenum-disulphide acts as a good lubricant at various temperature. Experiments were conducted to determine the friction factor, subsequently the true stress, true strain curves were developed to ascertain the K and n value's. Further, the ANSYS 8.0 software was used to simulate the experimental conditions using power law. The finding indeed gives clear clarification that the variation of inner diameter between physical modeling and Finite Element model is less than 8%.

Keywords: Aluminium, alloys, ring-compression test, power-law, friction coefficient, finite Element Analysis.

1 Introduction

Aluminium alloys have been used in advanced applications because of their combination of high strength, low density, durability, machinability and cost. These properties makes it very attractive compared to other materials. There are many areas where these aluminium alloys can be successfully put in to use such as constructing aircrafts, wheels, roofing materials, sport goods etc [Evangelista, Forcellese, Gabrielli, and Mengucci (1990)]. Aluminum alloys are treasure of noted properties that make them a perfect choice for different industrial applications. Some of these properties are i) Non heat treatable ii)Hardness iii) Corrosion resistance iv) Ductility. The aluminum alloys(Al-4Mg) can be converted into any form as they are ductile in nature. They can be drawn into various shapes such as wires sheets without any inconvenience. The forging of metal powder components having difficult shapes and curves is the latest and rapidly growing technique in the metal working technology.Hence, in metal forming industries, utmost care is to be given to determine the durability of die, formability of work material which is being influenced by coefficient of friction [Ebrahimi and Najafizadeh (2004)]. Since excessive friction leads to heat generation, wear galling of the tool-surface contributed significant Premature failure of tools,it demands more investigations in metal forming industries to asses the effect of friction factor. Moreover, most of the studies were aimed at determining the mechanical properties of the aluminium alloy Viz., young's modulus, yield point, elongation, tensile strength and compressive strength. Nevertheless, the other parameters of the stress-strain curves (flow curve), such as strain-hardening exponent (n) and strength coefficient (k), termed as flow properties, have not been discussed in detail. These parameters play a vital role in analyzing the plastic deformation of porous materials [Dieter (1988); Senthilvelan, Venkatraman, and Raghukandan (2000)]. While examining the hot working processes, the flow stress of material at elevated temperatures is one of the indispensable information to have knowledge on the deformation mechanism.Ring compression test is commonly employed technique to determine these formability parameters mainly due to is simplicity [Senthilvelan, Venkatraman, and Raghukandan (2000)]. Considering the aforementioned aspects, the present investigation has been aimed at the determination of friction coefficient, strength coefficient and strain hardening exponent. The experimental results have been compared with the values obtained by Finite Element Analysis.

2 Processing of Aluminium Alloys by Powder Metallurgy

To fabricate Al-4Mg alloys, Powder Metallurgy (P/M) and conventional ingot metallurgy, including infiltration technique are the methods commonly employed. Among them Powder metallurgy technique has major advantage over other technique due to ease of convenience to obtain homogeneous distribution of properties especially in the manufacture of high-temperature materials (refractory vessels), self-lubricating bearings, gears etc [Senthilvelan, Venkatraman, and Raghukandan (2000); Doraivelu, Gegel, Gunasekera, Malas, and Morgan (1984)]. The process of producing powder metallurgy components using powder metal forging is basically a combination of two conventional processes, namely powder metal fabrication processes(P/M) and forging. The Powder metallurgy components are being widely used for sophisticated industrial applications. This technique is used for material systems that are hard to machine and difficult to cast due to complex solidification behavior of material chosen. The worldwide popularity of powder metallurgy lies in the ability of this technique to produce such detrimental shapes with exact dimensions at a very high rate production and low cost [Senthilvelan, Venkatraman, and Raghukandan (2000)]. Hence, P/M has been chosen to process Aluminium alloy.In this present investigation atomized aluminium powder and Mg powder of 4% were procured from M/s, The Metal Powder Company, Madurai, India. The aluminium powder was analyzed for its purity and was found to be 99.7% pure with 0.3% insoluble impurities. The aluminium - 4% Mg entire surfaces of the compacts were coated with the special ceramic slurry to avoid oxidation during sintering. The ceramic coated compacts were dried at the ambient conditions for a period of 12 h and sintered at the temperature of 530°C for a period of 60 *min* in an electric muffle furnace, and then the sintered compacts were cooled inside the furnace chamber itself till they attain room temperature. Powder blend was used for the preparation of compacts of height at 6.6 *mm*.The prepared sintered compact in this investigation is shown in fig. 1.

Figure 1: Sintered Ring Preforms

3 Experimental Details

The ring compression test is carried out in order to measure the coefficient of friction,particularly for bulk deformation processes [Senthilvelan, Venkatraman, and Raghukandan (2000)]. In this test, a flat ring is compressed to a predetermined strain between two flat platens The compression tests were carried out in a ENKAY hydraulic universal testing machine at a speed of 0.05 mm/s.The outer diameter: inner diameter: height ratio was kept at approximately 6 : 3 : 2 which is followed in a ‘standard’ ring-compression-test [Rao (1993)] to facilitate the measurement of friction. By considering the standard proportions ratios, the outer diameter of the specimens has been taken as 20 *mm* and inner diameter as 10 *mm* with initial height of 6.6 *mm*. The experiments were carried out at temperature of 303K (room temperature), 523K, 773K at a displacement of 4 *mm* without lubricant, with SAE 40 oil, Molybdenum Disulphide, graphite. The true stress-strain data have been recorded by computer system which is enabled with WINCOM software through Universal Testing machine. Fig. 2, 3, 4, shows the load-displacement curve in different friction conditions. From these recorded diagrams, true stress and true strain values were determined and thus obtained curves were shown in Fig 5, 6 and 7.

After every test, the dimensions of each sample had been measured to ascertain the ratio of change in inner diameter to height. From the observation, it is found that the inner diameter of the ring is decreases as the interfacial friction whereas the inner diameter increases for low interfacial frictional conditions. Thus the changes in the internal diameter of the compressed ring are sensitive to friction at the die-work piece interface.

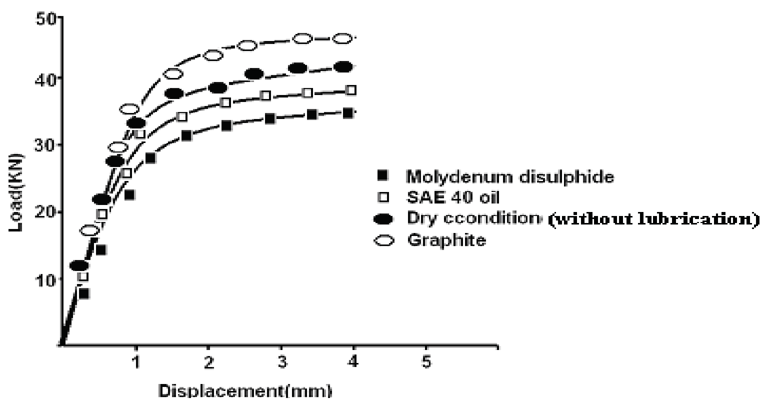

Figure 2: Load-Displacement curve at Room Temperature (323*k*)

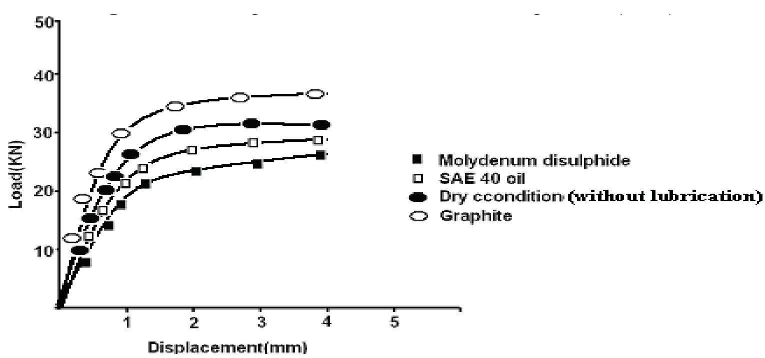

Figure 3: Load-Displacement curve at Room Temperature (473*k*)

4 Analytical Approach

The mathematical expressions used for the determination of various upsetting parameters', namely, stress, strain, the strain hardening exponent and strength coefficient for various unlubricated conditions at different temperatures. The method

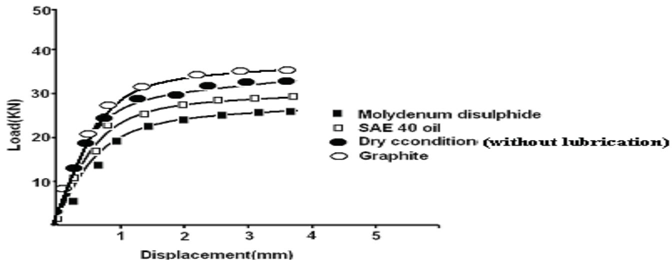

Figure 4: Load-Displacement curve at high Temperature (773*k*)

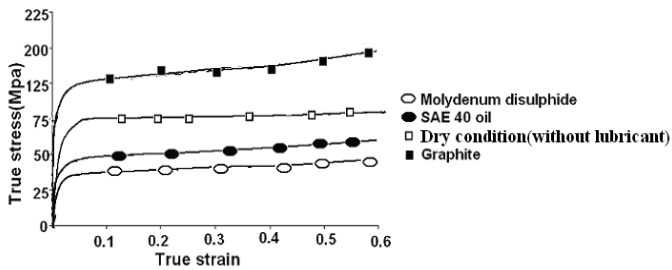

Figure 5: True stress-True strain curve at Room Temperature (323*k*)

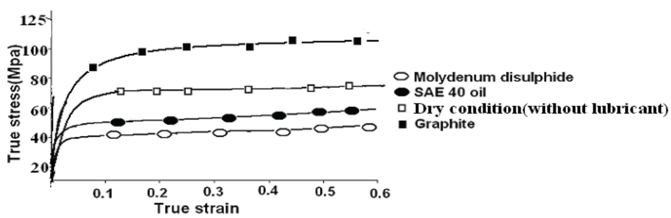

Figure 6: True stress-True strain curve at warm Temperature (473*k*)

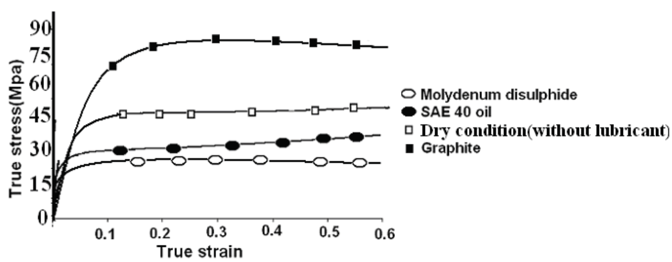

Figure 7: True stress-true strain curve at high Temperature (773*k*)

of determining the flow parameters such as k and n are adopted from the earlier research finding [Narayasamy, Ramesh, and Pandey (2007)] and briefly illustrated below:

$$\text{True stress}(\sigma) = \text{intaneneous load}/\text{instanteneous Area}$$

where σ is the axial stress

The axial true strain (ε) is expressed as given below:

$$\varepsilon = \ln(h_o/h_f) \tag{1}$$

where h_o is the initial height of P/M preform before deformation and h_f is the height of the preform after deformation. The strain-hardening exponent value (n) and the strength coefficient (k) were determined from the Power law [Dieter (1988)]

$$\sigma = k\varepsilon^n$$

It is assumed that the consecutive compressive loads were specified as elsewhere [Senthilvelan, Venkatraman, and Raghukandan (2000)] $1,2,3,\ldots,(m-1),m$. Now the above equation can be rewritten as:

$$\sigma_{(m-1)} = k((m-1))^n \tag{2}$$

$$\sigma_m = k(\varepsilon_m)^n \tag{3}$$

Subtracting Eq. (2) from Eq. (3), the following expression can be obtained

$$(\sigma_m - \sigma_{(m-1)}) = k[(\varepsilon_m)^n - (\varepsilon_{(m-1)})^n] \tag{4}$$

Above equation can be rearranged as follows

$$k = \left[\frac{(\sigma_m - \sigma_{(m-1)}}{[(\varepsilon_m)^n - (\varepsilon_{(m-1)})^n]}\right] \tag{5}$$

Now dividing equation (2) by (3) we get

$$(\sigma_m/\sigma_{(m-1)}) = (\varepsilon_m/\varepsilon_{(m-1)})^n \tag{6}$$

Taking natural logarithm on either side

$$\ln(\sigma_m/\sigma_{(m-1)}) = n\ln(\varepsilon_m/\varepsilon_{(m-1)}) \tag{7}$$

Strain hardening exponent can be obtained as follows

$$n = \frac{\ln(\sigma_m/\sigma_{(m-1)}}{\ln(\varepsilon_m/\varepsilon_{(m-1)}} \tag{8}$$

5 Results and Discussion

5.1 Effect of temperature

The parameters and variables that affect the interfacial friction factor $[\mu]$ involve the material, the surface condition, the temperature, the strain rate, the geometry of the specimen and so on [Rao (1983)]. Amongst them, the thermal conductivity of the material plays vital role in generating the interface the between the die and wokpiece which is governed by the process Temperature. As the thermal conductivity of aluminum alloy has paramount influence on the dissipation of heat extensively [Evangelista, Forcellese, Gabrielli, and Mengucci (1990)], it is necessary to know the effect of temperature in determining the friction factors. From Fig. 8(a,b,c,d) it is observed that as temperature increases, friction factor also increases, irrespective of the lubricant employed.This condition prevails in all processing route such as conventional ingot and P/M.IN specific p/m has the advantage of changing the density which influence the friction factor, can explore variation in magnitude of friction factor as stated by the researchers [Venugopal, Venkataraman, Vasudevan, and Padmanabhan (1988)]. The findings of increase in friction factor with increase in temperature has concurred with investigations done by earlier researchers [Li, Peng, Liu, and Liu (2001)].

The reason could be that the lubricant used for analysis loses its performance during high temperature [Li, Peng, Liu, and Liu (2001)]. Due to this effect, the material - tool interface acts as a dry lubrication condition which eventually increases friction factor. Moreover, the increase in temperature leads to the increase in shear stress of the specimen-die interface as altered by Li, Peng, Liu, and Liu (2001). From the equation stated below shows that friction factor is influenced by shear stress of lubricant (τ_s) and inversely proportional to the strength of the specimen(k).

$$M = \tau_s/k$$

On the contrary to the aforesaid finding, the friction factor decreases with increase in temperature when the inorganic thermoplastic polymer of spatial network structure (glass) is used as a lubricant [Li, Peng, Liu, Liu, and Jiang (2000)]. As in the case of lubricant such as SAE 40 oil, Molydenum disulphide and graphite have not been stated as thermoplastic polymer in the literature available, it is emphasized that friction factor increase with increase in temperature [Li, Peng, Liu, and Liu (2001)]. Further, Investigations had been carried out pertaining to the heat generated by adiabatic heating and the friction between the sample surfaces and the dies, as well as the heat loss through conduction between the sample and the dies [Zhao (1993)]. It is concluded that effect of heat generated from the friction between the dies and sample surfaces is fairly significant when lubrication between the die and

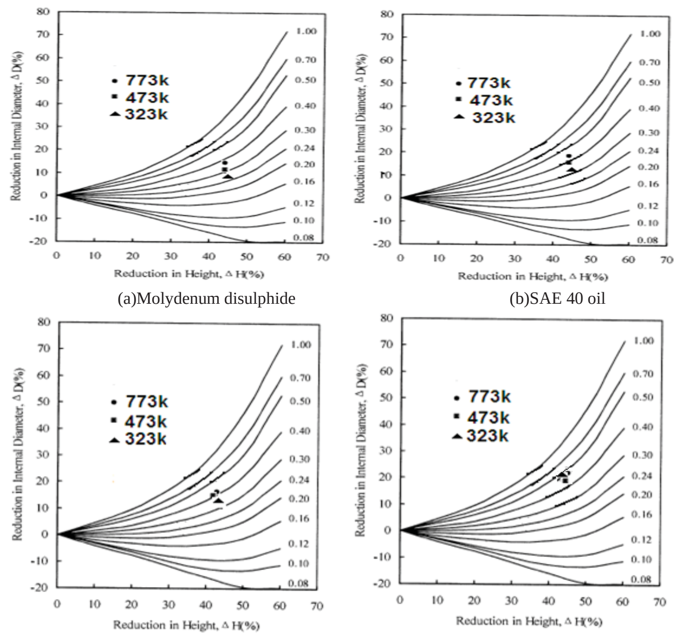

(a)Molydenum disulphide (b)SAE 40 oil

(c)Graphite (d) No lubricant

Figure 8: Experimental results of ring compression test using different lubricant

the sample surfaces fairly good. Hence the effect of temperature on friction factor is an interrelated property of lubricant used.

5.2 Effect of lubricant

Lubricant plays decisive role as in case of determining the friction factor [Malayappan and Narayanasamy (2003)]. The Present research work comprises application of lubrication such as SAE 40oil, graphite, Molydenum disulphide, dry condition at different temperature. Among the various lubricant, molybdenum disulphide possesses good lubrication with friction factor of 0.26 [Li, Peng, Liu, Liu, and Jiang (2000)]. Peterson, Martins, and Bay (1998) similarly, justified that MoS2 act as a good lubricant with the value of 0.32 in which commercial aluminium has been used as base material. The reason stated in their discussion that application of molybdenum disulphide leads to loss of contact between tool and workpiece interface which subsequently leads to reduction in the pressure generation. Hence the total force given is utilized with maximum and transferred further to the the specimen. However, in case of dry lubricant such a trend trend does not exist as there is contact between tool and interface. Further from other findings [Rao (1983)], the similar observation has been defended with the reason that viscosity of different lubricant influences the friction factor. As the resistance offered at the interface accelerates the bulging of internal diameter, the percentage reduction significantly increases, paves the way to increase in friction factor. The friction factor from different lubricant is shown in the Table. 1. This reason has been verified from the current findings since viscosity of molybdenum disulphide is at least in comparison with other lubricant.The concurrent trend has been prevailed when Malayappan and Narayanasamy (2003) attempted in their investigations where aluminium was used as a base material.As far as the characteristics of graphite is concerned, it is independent with respect to the specimen used for compression test. Hence such a lubricant draws attention of the researchers [Li, Peng, Liu, and Liu (2001)] to determine the friction factor.

6 Validation of FEA results

The specimen with ratio of standard ring compression test i.e $(6:3:2)$ has been taken for modeling as stated in the experimental procedure and subsequently deformation test is carried out under the dry conditions and lubricated conditions with lubricants such as SAE40oil, graphite, Molydenum disulphide by using ANSYS 8.0 software. The outcome of the experimental results i.e the values of friction factor of different lubricants had been given as one of the input parameters and further the simulation was preformed to evaluate the percentage reduction of inner diameter in comparison with the conventional procedure. In the methodology of FEA, as suggested by the researchers [Rao, Kamaluddin, Appao, Rao, and N. R. M. R. Sarcar (2009)] the tetrahedral element with 10-node(solid 92 in Ansys 8.0 library) of element size which reduces the number of iteration had been chosen and the specimen geometry was neither too meshed nor coarse meshed. such that long computational time and accuracy with unnecessary precession was minimized.Furthermore, the nature of the loading is uniaxial compression,the non-cyclic with absence of bauschenr effect,.As emphazised by different researchers, the Power law has been accommodated with isotroic hardening flow rule where the strength coefficient(k) and strain hardening effect(n) controls the flow of the deformation. The k-value and n-value of alluminium alloy(Al-4Mg) at different temperature was taken from the experimental findings. The percentage reduction in height of 42% was given and subsequently the percentage reduction of inner diameter was consider as response to verify with the experimental observation. The dimensional changes of the inner diameter of the rings were taken from the middle of the ring specimen in both physical model and simulation to avoid the barreling effect ,specifically ,in high friction conditions since the middle and edge are different as suggested by the researchers [Robinson, Ou, and Armsrong (2004)]. The observation reveals that there is less than 8% of variation in inner diameter between the physical modelling from experiment and finite element modeling at different temperature as depicted in figures. 9, 10, 11 and 12.

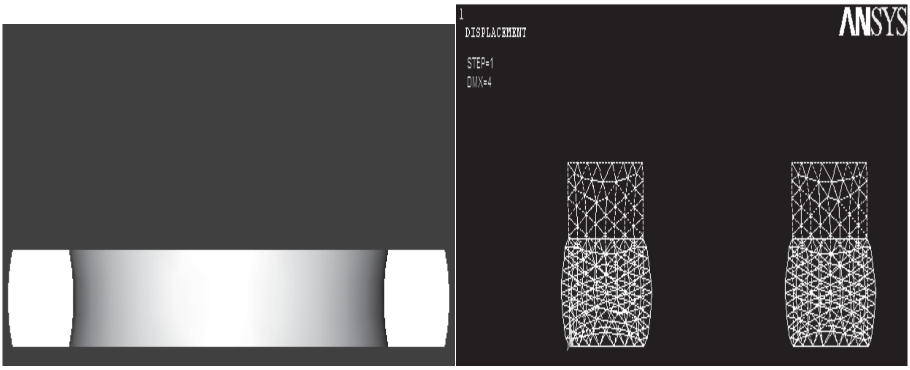

a) Deformation of physical model at 303k b)Deformation of FE Model at 323k

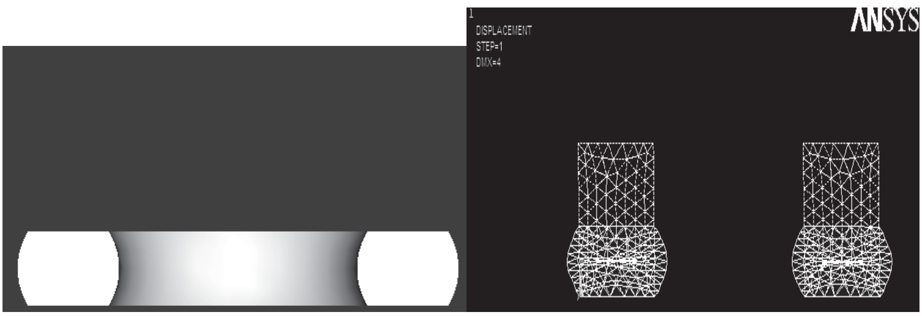

c) Deformation of physical model at 450k d)Deformation of FE Model at 473k

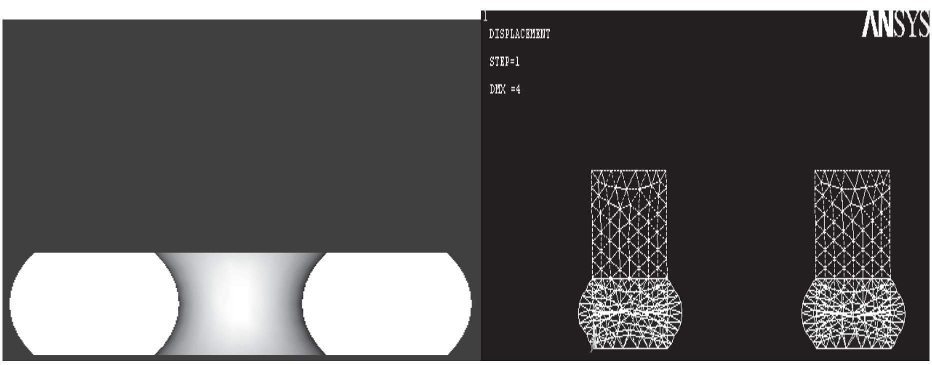

e)Deformation of physical model at 703k f)Deformation of FE model at 773k

Figure 9: Samples of deformed ring preforms at different temperature using Molybdenum disulphide as lubricant

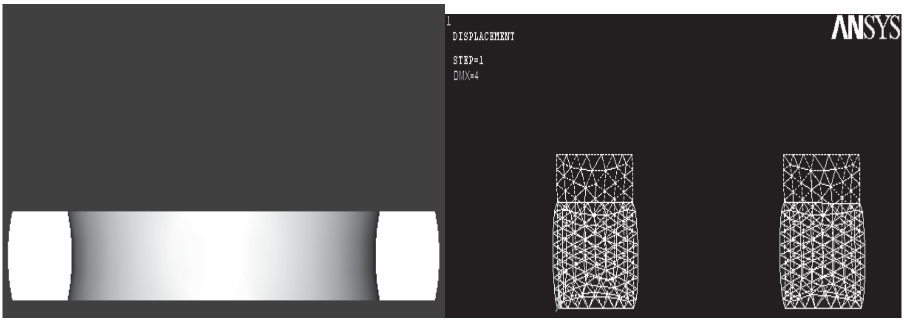

a) Deformation of physical model at 303k b)Deformation of FE Modelat 323k

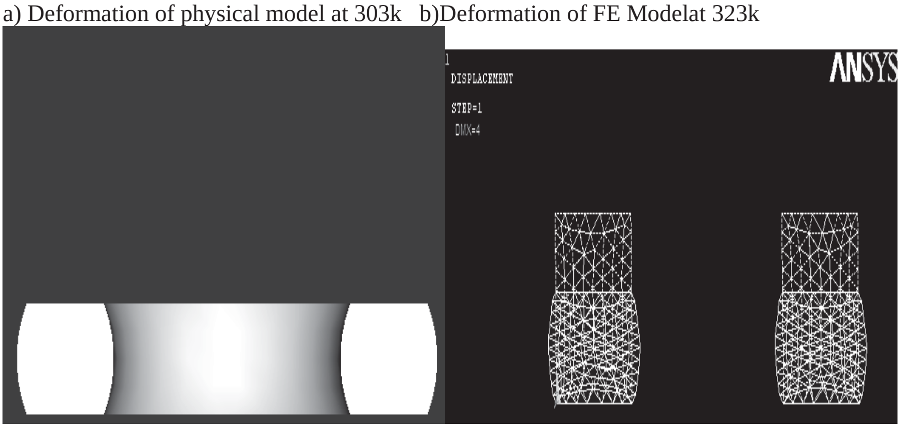

c) Deformation of physical model at 450k d)Deformation of FE Modelat 473k

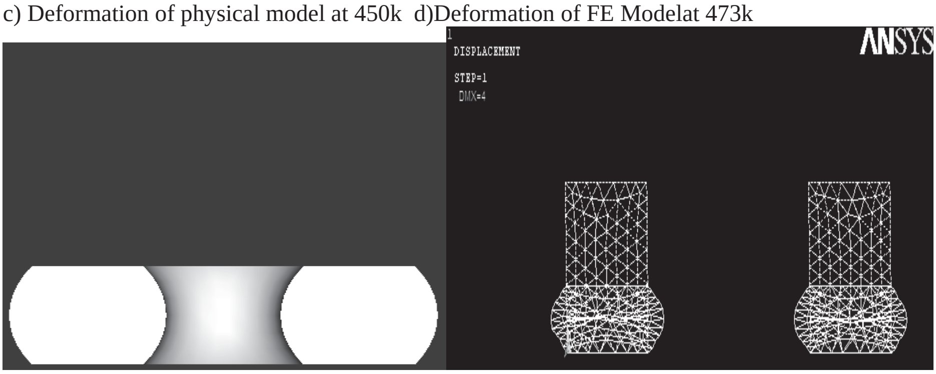

e) Deformation of physical model at 703k f)Deformation of FE Modelat 773k

Figure 10: Samples of deformed ring preforms at different temperature using SAE 40 oil as lubricant

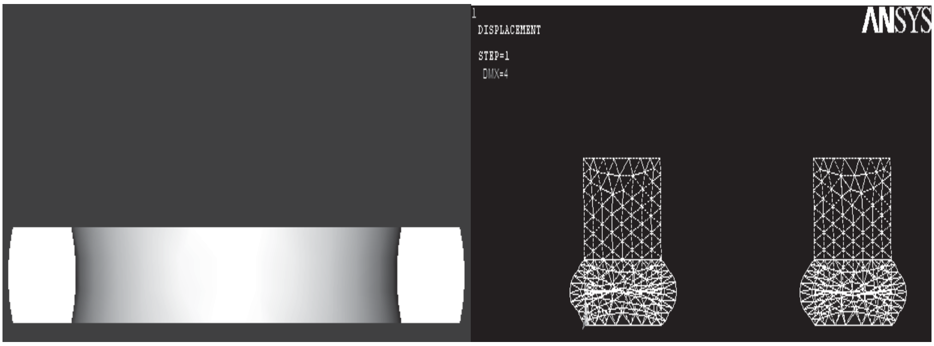

a) Deformation of physical model at 303k b)Deformation of FE Model at 323k

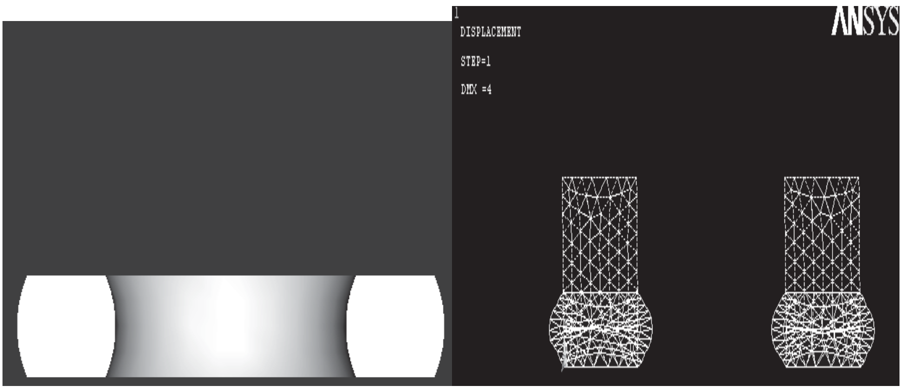

c)Deformation of physical model at 450k d)Deformation of FE Model at 473k

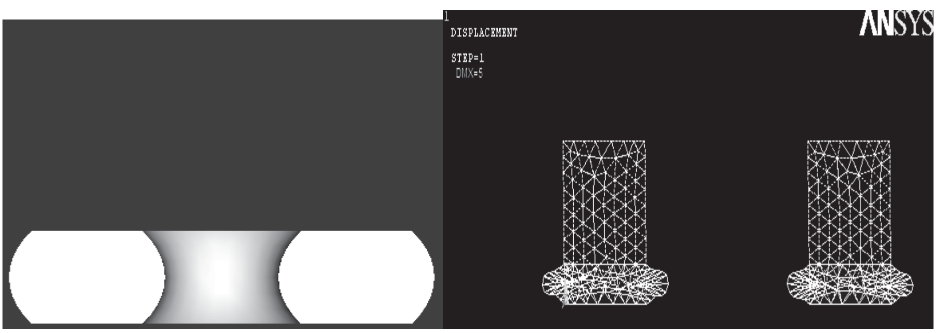

e) Deformation of physical model at 703k f)Deformation of FE Model at 773k

Figure 11: Samples of deformed ring preforms at different temperature using graphite as lubricant

a) Deformation of physical model at 303k b)Deformation of FE Model at 323k

c)Deformation of physical model at 450k d)Deformation of FE Model at 473k

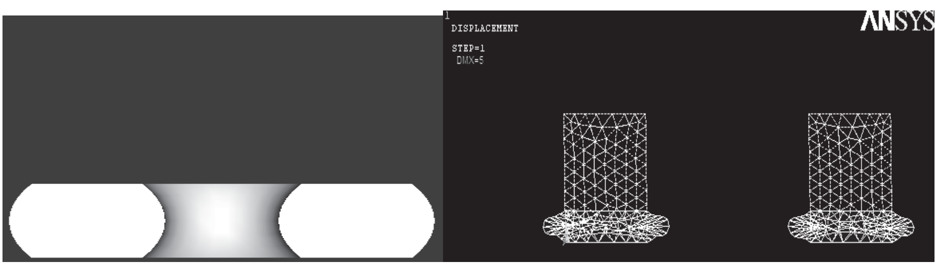

e) Deformation of physical model at 703k f)Deformation of FE Model at 773k

Figure 12: Samples of deformed ring preforms at different temperature at dry condition

The stress distribution across the specimen at each test is represented in the figures 13, 14, 15, 16 support the findings of experimental values. Hence this solution can be used to determine the the friction factor executed in prescribed condition (lubricant, temperature) without running out real time experiment which consumes time, energy, material.

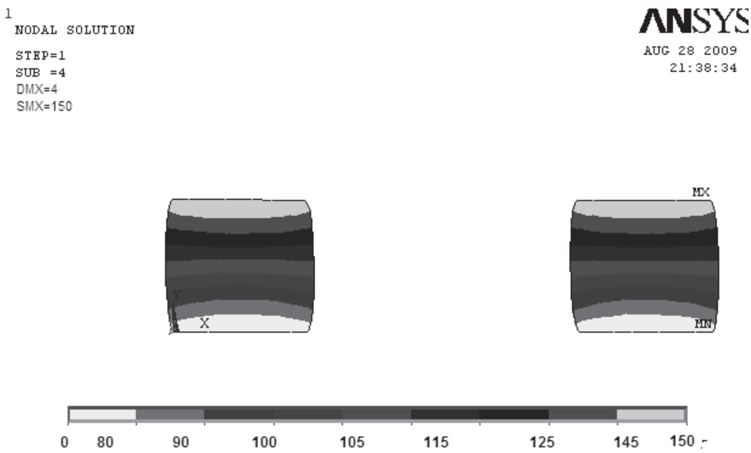

a)stress distribution of FE Modelat 323k

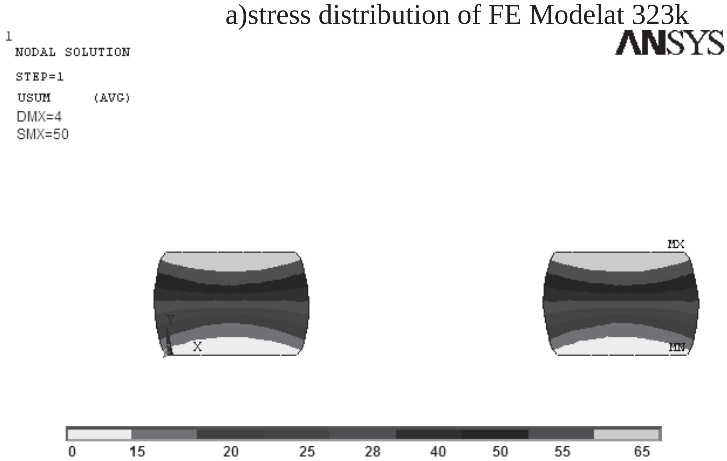

b) stress distribution of FE Modelat 473k

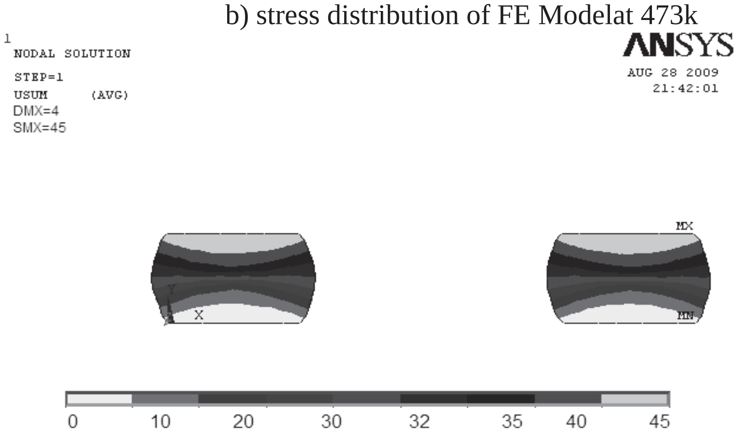

c) stress distribution of FE Modelat 773k

Figure 13: Stress distribution of FE model at different temperature using Molydenum disulphide

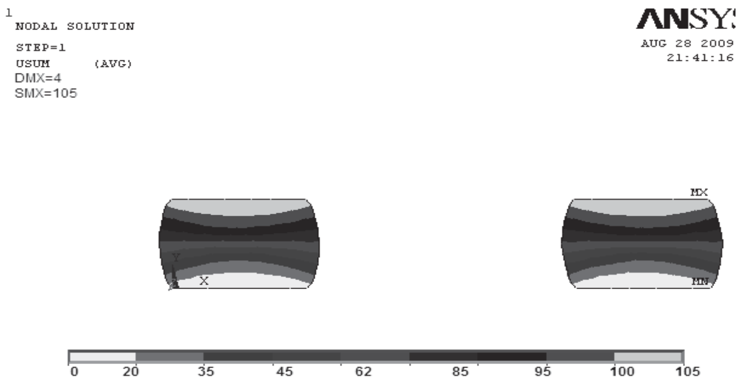

a) stress distribution of FE Modelat 323k

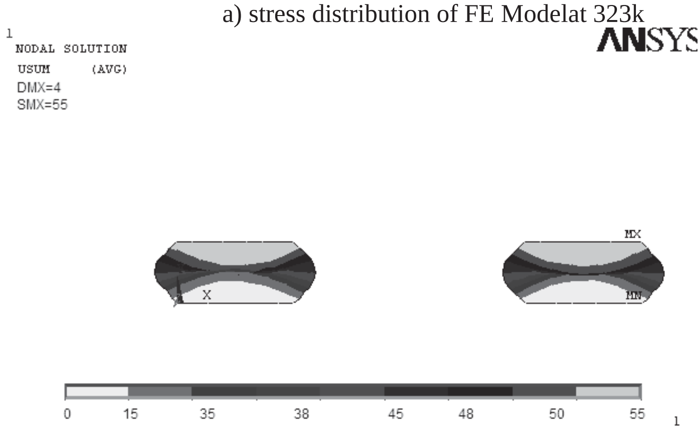

b) stress distribution of FE Modelat 473k

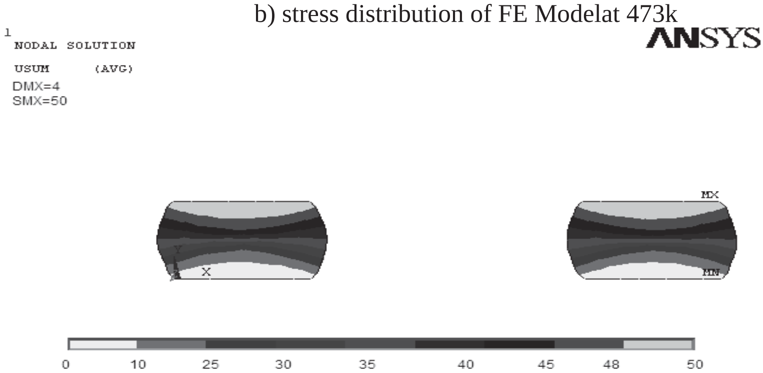

c) stress distribution of FE Modelat 773k

Figure 14: Stress distribution of FE model at different temperature using SAE 40 oil as lubricant

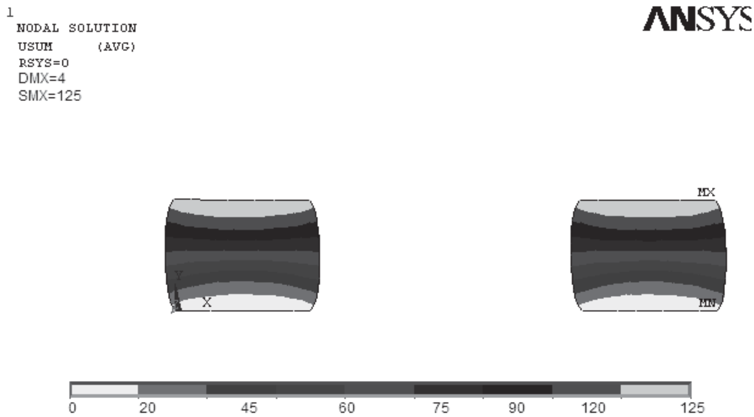

a) stress distribution of FE Modelat 323k

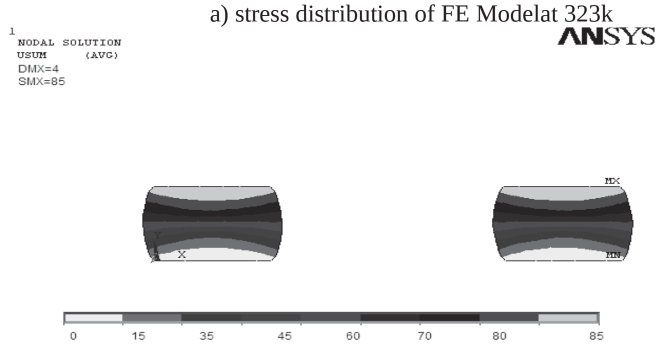

b) stress distribution of FE Modelat 473k

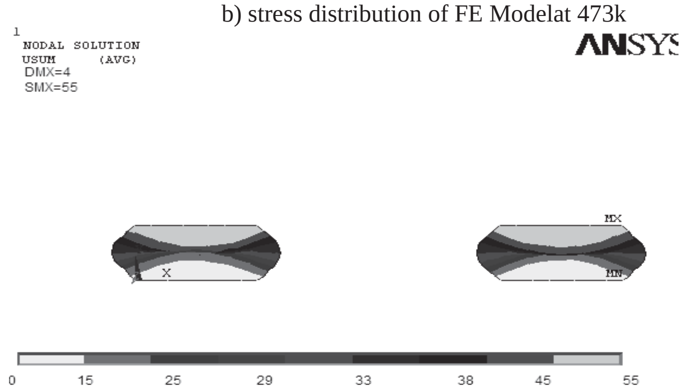

c) stress distribution of FE Modelat 773k

Figure 15: Stress distribution of FE model at different temperature using Graphite as lubricant

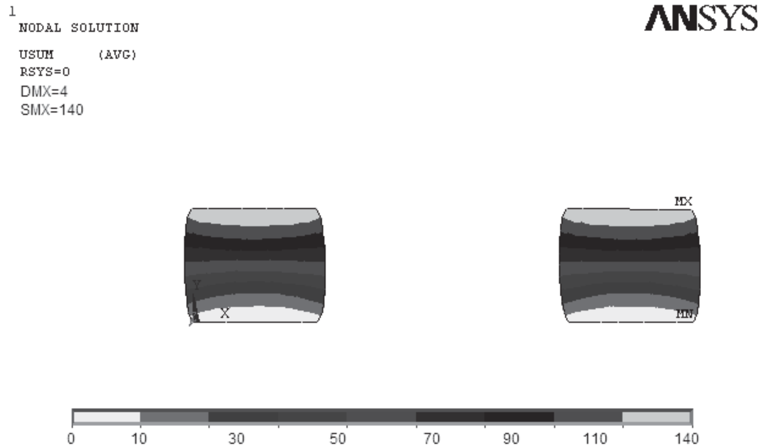

a) stress distribution of FE Model at 323k

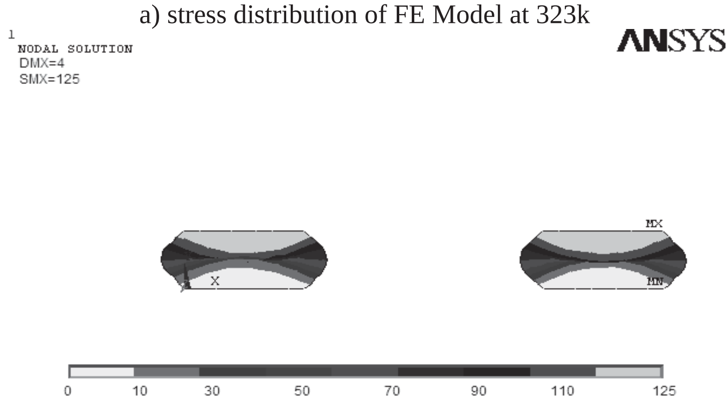

b) stress distribution of FE Model at 473k

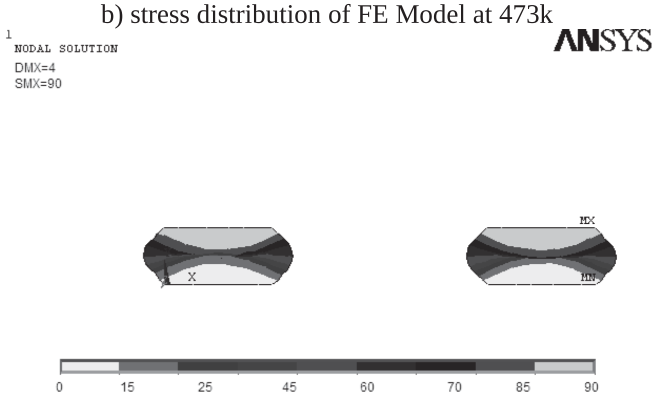

c) stress distribution of FE Modelat 773k

Figure 16: Stress distribution of FE model at different temperature in dry condition

In specific the methodology is best suited for unconventional processing route such as Powder metallurgy with different K-value and n-value changes as these influencing parameters are unavailable. Finite element analysis gives stress distribution across the preform at various conditions suggest that stress distribution is maximum at the edges as there is a intersection between two areas which is perpendicular to each other [Liu, Zhang, Hu, Wang, Wang, Huang, and Tang (2004)].

7 Conclusion

The influential parameters such as lubricant, temperature to determine the coefficient of friction has been analyzed vividly to evaluate its significance. Among the Lubricant, Molydenum disulphide act as a efficient lubricant in various temperature followed by SAE 40oil, graphite, dryconditions as earlier studies on viscosity supports this findings. In dry conditions, the friction factor is more when compared with lubricated condition under various temperatures as observed from other findings. The effect of temperature shows discrepancies in the magnitude of friction factor as performance of lubricant is lost at high temperatures. The investigation has been extended to study the barreling effect. The radius of curvature of the barrel obtained from experimental work concurs well with the calculated values and barreling radius determined from Finite Element Analysis found to be closer with the experimental findings. Moreover, Finite element analysis gives more realistic with physical results leading to evaluate friction factor with variation of only less than 8%.

References

Dieter, G. E. (1988): *Mechanical Metallurgy*. McGraw-Hill Book Company, London, UK.

Doraivelu, S. M.; Gegel, H. L.; Gunasekera, J. S.; Malas, J. C.; Morgan, J. T. (1984): A new yield function for compressible p/m materials. *Int. J. Mech Sci*, vol. 26, pp. 527–35.

Ebrahimi, R.; Najafizadeh, A. (2004): A new method for evaluation of friction in bulk forming process. *J. Mat. Proces. Technol*, vol. 152, pp. 136–143.

Evangelista, E.; Forcellese, A.; Gabrielli, F.; Mengucci, P. (1990): Hot formability of al 6061 p/m aluminium alloy. *Journal of Material Processing Technology*, vol. 24, pp. 323–332.

Li, L. X.; Peng, D. S.; Liu, J. A.; Liu, Z. Q. (2001): An experimental study of the lubrication behavior of graphite in hot compression test of ti-6al-4v alloy. *J. Mat. Proces. Technol.*, vol. 112, pp. 1–5.

Li, L. X.; Peng, D. S.; Liu, T. A.; Liu, Z. Q.; Jiang, Y. (2000): An experimental study of the lubrication behavior of a5 glass lubricant by means of the ring compression test. *J. Mat. Proces. Technol.*, vol. 102, pp. 138–142.

Liu, G.; Zhang, L. B.; Hu, X. L.; Wang, Z. R.; Wang, R. W.; Huang, S. D.; Tang, Q. B. (2004): Applications of numerical to the analysis of bulk-forming processes-case studies. *J. of Material Processing Technology*, vol. 30, pp. 56–61.

Malayappan, S.; Narayanasamy, R. (2003): Some observation on barreling of aluminium solid cylinders during cold upsetting using different lubricants. *Mater Sci Technol*, vol. 19, pp. 1705–1708.

Narayasamy, R.; Ramesh, T.; Pandey, K. S. (2007): An experimental investigation on strain hardening behavior of aluminium - 3.5% alumina powder metallurgy composite preform under various stress states during cold upset forming. *Materials & Design*, vol. 28, pp. 1211–1223.

Peterson, S. B.; Martins, P. A. F.; Bay, N. (1998): An alternative ring-test geometry for the evaluation of friction under low normal pressure. *J. Mat. Proces. Technol.*, vol. 79, pp. 14–24.

Rao, J. B.; Kamaluddin, S.; Appao, J.; Rao, M. M. M.; N. R. M. R. Sarcar, N. (2009): Finite element analysis of deformation bahaviour of aluminium-copper alloys. *Materials and Desgin*, vol. 30, pp. 1298–1309.

Rao, K. P. (1983): *Deformation processing and kinetics of hot working in aluminum alloys*. Ph.d thesies, IIT, Madras, India, 1983.

Rao, K. P. (1993): A review of ring compression testing and applicability of calibration curves. *J. Mat. Proces. Technol.*, vol. 37, pp. 295–318.

Robinson, T.; Ou, H. C.; Armsrong, G. (2004): Study on ring compression test using physical modeling and fe simulation. *J. Mat. Proces. Technol.*, vol. 153-154, pp. 54–59.

Senthilvelan, T.; Venkatraman, A.; Raghukandan, K. (2000): Evaluation of formability properties of p/m copper preforms at elevated temperature. *Key Engineering Materials*, vol. 183-187, pp. 1273–1278.

Venugopal, P.; Venkataraman, S.; Vasudevan, R.; Padmanabhan, K. A. (1988): Ring-compresion test on sintered iron performs. *J. Mech.Work.Technol.*, vol. 16, pp. 51–64.

Zhao, D. (1993): Temperature correction in compression tests. *J. Mat. Proces. Technol.*, vol. 36, pp. 467–471.